DESIGN AND CHARACTERIZATION OF RUTAECARPINE-LOADED CHITOSAN NANOPARTICLES

Tanguturi Arun Kumar[a], P. Geetha[b]*

Article History: **Received**: 29.05.2022 **Revised**: 28.06.2022 **Accepted**: 28.07.2022

Abstract: Rutaecarpine found to have anti cancer properties. The compound is well-tolerated with low toxicity profile but its clinical translation against cancer is limited due to poor dissolution characteristics, and substantial first-pass metabolism. Objective: This paper deals with the preparation, optimization and characterization of Chitosan nanoparticles encapsulating Rutaecarpine for its intended use as anticancer formulation. Methods:. A number of variables such as organic solvent, its ratio with aqueous phase, drug to polymer ratio, mixing speed were optimized. To investigate the effect of process variables on mean particle size, drug loading and entrapment efficiency of several stabilizers were also screened. In vitro Rutaecarpine release was studied using dialysis bag method. Final formulation was freeze dried for long term storage for which a number of lyoprotectants were screened. Results: It was observed that stabilizer, solvent, drug to polymer ratio, surfactant concentration, organic/aqueous phase volume ratio and stirring speed influence nanoparticle size significantly whereas drug loading and entrapment efficiency were significantly influenced by stabilizers, solvents, drug to polymer ratio and surfactant concentration. Optimized parameters were chitosan and TPP concentration 0.5 mg/ml, chitosan to TPP ratio 4:1, magnetic stirring at 1000 rpm just for five minutes was found to be sufficient.. So, based on in vitro characterization and lyophilization of all the Rutaecarpine nanoparticulate formulations based on natural biodegradable polymers, folic acid coated chitosan nanoparticles were found to be the best for encapsulation of Rutaecarpine and was selected for in vitro anticancer study.

.

Keywords: PLA, Rutaecarpine, polymeric nanoparticles, emulsification solvent diffusion method.

[a]. Research Scholar, School of Pharmaceutical Sciences, Vels Institute of Science technology and advanced studies

[b]. Department of Pharmacy Practice, School of Pharmaceutical Sciences, Vels Institute of Science Technology and Advanced Studies, Pallavaram, Chennai, India

***Corresponding author**

Email: lgeethapharma@Gmail.com

DOI: 10.31838/ecb/2022.11.05.001

INTRODUCTION

Drug delivery is a general term that refers to formulation and administration of a pharmacologically active compound for the purpose of providing an efficient drug plasma concentration, as well as bringing the drug to the specific site of action. Different strategies have been employed to overcome some drug stability issues in the gastrointestinal tract (GIT), control the drug release, enhance the transmucosal absorption, as well as get the drug into its site of action. Microfabrication is a technique that creates materials in the micrometer scale feature and has been reported to significantly improve diagnosis and biomedical applications. Modification of the material shape, surface characteristics, and release kinetics is a consequence of this micronization(1). Nanotechnology has been utilized as one of these strategies in the development of novel drug delivery systems through entrapment of the drug in nanoparticulate systems(2). In general, the potential applications of nanotechnology render this field an area of interest to many researchers and scientists. These applications have covered different scientific areas that extend from electronics to cosmetics(3-5).

Polymers obtained from natural origins have been extensively employed not only in the food industry but also in pharmaceutical technology. Polysaccharide polymers have emerged as being one of these because they are less toxic, biocompatible, and biodegradable(6). Incorporation of the therapeutic agent into a polymeric matrix, particularly of a natural origin, might potentiate the protection of the biologically active compound from degradation, control drug release, improve absorption, enhance the therapeutic effect, and lead to the consequential decrease in the frequency of administration. Chitosan, alginate, and carrageenan are the most commonly used polysaccharide polymers in various pharmaceutical applications(7). Chitosan is a polymer of interest that has been widely used for delivery of different therapeutic agents, particularly those based on chitosan micro- and nanoparticles, owing to its unique properties. Preparation of mucoadhesive formulations, enhancing the dissolution rate especially for poorly water-soluble drugs, utilization in drug targeting, and improvement of protein absorption are common therapeutic applications of this naturally occurring polymer(8).

MATERIALS AND METHODS

Materials

Rutaecarpine was obtained as a gift sample from Deccan Phytochemicals, Secunderabad, A.P., India. Poly(methacrylate) Chitosan were gifted by Evonik industries, Mumbai, India. Poly(d,l-lactide-co- glycolide acid) (PLGA),

with a copolymer ratio of dl- lactide to glycolide of 50:50 and 75:25 were purchased from Sigma Aldrich. All organic solvents of LR grade used were purchased from Sigma Aldrich.

CHITOSAN NANOPARTICLES

Preparation and optimization of Rtc-loaded chitosan nanoparticles

Chitosan nanoparticles (Ch-NP) were prepared by ionic gelation of chitosan with sodium tripolyphosphate (TPP) aqueous solution [9]. Chitosan was dissolved in aqueous acetic acid solution (1% w/v). Aqueous solutio of TPP was drop wise in to 10 ml chitosan solution under magnetic stirring at room temperature. chitosan nanoparticles were formed spontaneously upon incorporation of TPP solution under agitation with stirring. Rutaecarpine was added to the chitosan solution to get Rutaecarpine loaded Ch-NP. Different formulation and process variables were optimized by varying one variable at a time and keeping other variables constant.

Surface-modification of chitosan nanoparticles

Alginate coated chitosan nanoparticles (Alg-CS-NP)

Alginate coating on optimized chitosan nanoparticles was carried out in accordance with the method reported by Li et al. (2008), with slight modification. Solution of sodium alginate was pre-pared in phosphate buffer (10 mg/mL). Rutaecarpine loaded chitosan nanoparticles suspension (0.5%, w/v; pH 5.5) was added drop wise into alginate solution under mild agitation for 10 min followed by centrifugation at 3500 rpm for 5 min. The supernatant so obtained was discarded and alginate coated nanoparticles were resuspended into aqueous solution of calcium chloride to cross-link the alginate layer present on the surface of chitosan nanoparticles. The collected products were washed with purified water, centrifuged and freeze dried[8].

Folic acid coated chitosan nanoparticles (FA-CS-NP)

5mg folic acid was dissolved in 10mL 20% aqueous solution of sodium hydroxide and then dropped into 10mL phosphate buffer suspension (pH 7.4) containing 20mg of CS NP under oscillation for 30 min, followed by centrifugation at 3500 rpm for 5 min. Residue obtained were washed 3-4 times with deionized water, centrifuged at 16000 rpm for 20min, and freeze dried[9].

Characterization of Rtc-loaded chitosan nanoparticles

Particle size and PDI: A light scattering particle size analyzer was used to measure the particle size and particle size distribution of the chitosan nanoparticles prepared. All samples were measured at least three times.

Zeta potential: Measurements of zeta potential are commonly used to predict the colloidal system stability. The zeta potential was determined using Nano ZS, Malvern Instruments, Malvern, UK.

Drug loading and entrapment efficiency

Freeze dried nanoparticles were dissolved in acetonitrile. Rutaecarpine in the solution were measured by UV-Visible spectrophotometer at 310 nm. Drug loading and entrapment efficiency of Rutaecarpine were calculated using followingequations:

$$\text{Drug Loading} \frac{\text{Amount of Drug in nanoparticles}}{\text{Amount of nanoparticles recovered}} \text{ X } 100$$

SEM characterization

Scanning electron microscopy observations were conducted to determine the morphology of surface coated chitosan nanoparticles. For SEM characterization, formulations were mounted on the stub and coated with gold using ion sputter. Electron microscopy of the coated samples was performed with a working distance of ~5 mm with acceleration of 10.0 kV and images at various levels of magnifications were captured.

Lyophilization of optimized formulation

For long-term stability, surface modified chitosan nanoparticles were lyophilized. For this, lyoprotectants were added at 5% (w/v) concentration and dissolved completely in the nanoformulation. These dispersions were freeze dried using bench top freeze dryer (SP Scientific, Gardiner, NewYork, USA).

In vitro drug release study

In vitro release of Rutaecarpine from the prepared chitosan nanoparticles was carried out by dialysis membrane method. Rutaecarpine loaded chitosan nanoparticles equivalent to 100 µg of Rutaecarpine were redispersed in 1 ml of dimineralized water in dialysis bags (sigma) with a molecular cut off of 12 kDA. The dialysis bag was suspended in 10 ml of release medium (pH 7.4 phosphate buffer with 0.3% tween-80) and placed in shaking water bath at 100 rpm maintained at 37°C. 100 µl of sample was withdrawn at predetermined time intervals and replaced with fresh medium. Finally samples were analyzed using validated UV-visible spectrophotometric method.

pH dependent stability study

Stability of freeze dried folic acid coated chitosan nanoparticles was assessed in different GIT pH and enzymatic conditions that can influence their physicochemical properties, drug release behaviour and can alter their stability characteristics during oral administration of the prepared formulation. pH dependent stability studies were carried out in following media (Table 1).

Table 1. Composition of GI fluids used to evaluate pH stability of folic acid coated chitosan nanoparticles

S.No.	GI fluids and pH	Composition
1.	pH 1.1	12 ml HCl (32%) in 1188 ml H_2O
2.	pH 3.5	150 ml solution (10.5 g citric acid+100 ml
		NaOH (1 M) + 395.5 ml H_2O) with 100 ml HCl
3.	pH 7.4	68 gNaH_2PO_4+ 15.6 g NaOH with 10 L H_2O
4.	Simulated Gastric Fluid (SGF)	0.2% NaCl, Pepsin0.7% HCl with pH 1.2

5.	Simulated Intestinal Fluid (SIF)	0.685 Monobasic Potassium Phosphate, 1% NaOH and 1% Pancreatin with pH 7.4

Briefly, 9 ml of simulated fluids were added to 1 ml of reconstituted folic acid coated chitosan nanoparticles. Particle size, PDI and entrapment efficiency were determined after the incubation time of 2 h for pH 1.1, pH 3.5 and SGF while 6 h for pH 7.4 and SIF.

Storage stability study of lyophilized formulation

To study the effect of the long-term storage on the physicochemical properties of the final optimized chitosan nanoformulation, glass vials containing lyophilized nanoparticles were closed with rubber stoppers, sealed with aluminium caps and stored at three different sets of temperature and humidity conditions. Storage conditions were selected based on ICH guidelines as follows: 2-8°C (refrigerated conditions), ambient conditions and 40°C/75% RH (accelerated conditions)[10].

Directly after lyophilization process and at predetermined sampling time points, the samples were withdrawn and analyzed for the changes in physicochemical properties that are likely to change during long-term storage and are likely to influence the quality, safety and efficacy of the product. The physicochemical properties studied include physical appearance, ease of reconstitution, particle size, polydispersity, zeta potential and drug retention.

Statistical analysis

The results are reported as mean ± standard deviation of triplicate measurements. Statistical analysis of the results was performed using one-way analysis of variance (ANOVA), followed by Dunnet's test in terms of particle size, drug loading and entrapment efficiency of Rutaecarpine nanoparticles. Student's t-test was applied when two groups were compared.

RESULTS AND DISCUSSION

Effect of formulation parameters on mean particle size, PDI, drug loadingand entrapment efficiency

i. Influence of chitosan concentration

Table 4.19 shows the influence of chitosan concentration from 0.5 mg/ml to 3 mg/ml on mean particle size, Rutaecarpine entrapment efficiency and drug loading. Initially the particle size decreased from 225.87 nm to 178.22 nm but then increased linearly to 503.00 nm. PDI also showed the same trend. Best PDI was obtained with 1 mg/ml concentration (0.15). On increasing chitosan concentration further PDI also increased to 0.55. Highest entrapment efficiency and drug loading was obtained at 1 mg/ml chitosan concentration i.e. 65.1% and 10.3%w/v respectively. On further increasing chitosan concentration Rutaecarpine entrapment efficiency decreased. So by varying chitosan concentration smallest size nanoparticles (i.e. 178.22 nm) were obtained at 1 mg/ml concentration, which also showed least PDI and highest entrapment efficiency and drug loading.

Table 2. Effect of chitosan concentration on particle size, PDI, drug loading (DL) and entrapment efficiency (EE) of chitosan nanoparticles

Concentration (mg/ml)	Size (nm)	PDI	DL (%w/v)	EE (%)
0.5$	225.87 ± 6.8	0.58 ± 0.02	4.6 ± 0.4	30.9± 1.5
1	178.22 ± 5.3*	0.15 ± 0.01	10.3 ± 0.5	65.1 ± 1.7*
1.5	359.15 ± 6.1*	0.20 ± 0.04	9.1 ± 0.6	60.3 ± 1.2*
2	437.53 ±9.9*	0.31 ± 0.07	5.9 ± 0.3	54.6 ± 2.2*
3	503.00 ± 12.9*	0.55 ± 0.09	5.5 ± 0.5	49.8 ± 1.5*

* p value< 0.05 when compared to control group $

Influence of TPP concentration

Tripolyphosphate (TPP) concentration was also varied from 0.5 mg/ml to 3 mg/ml (Table 4.19). Similar trend was found in particle size entrapment efficiency and drug loading as with chitosan concentration. Initially particle size decreased from 267.97 nm to 180.32 nm when TPP concentration was increased from 0.5 mg/ml to 1 mg/ml. On further increasing TPP concentration, particle size also increased linearly to 487.48 nm with 3 mg/ml TPP concentration. Entrapment efficiency also increased initially from 28.9% (with 0.5 mg/ml TPP concentration) to 64.9% (with 1 mg/ml TPP concentration). On further increase in TPP concentration entrapment efficiency decreased to 41.5% with 3 mg/ml TPP concentration. Therefore by varying TPP concentration smallest size nanoparticles were obtained with 1 mg/ml concentration i.e. 180.32 nm which also showed highest Rutaecarpine entrapment efficiency and drug loading of chitosan nanoparticles i.e. 64.9% and 10.1±0.7 %w/v.

Table 3. Effect of TPP concentrations on particle size, PDI, drug loading (DL) and entrapment efficiency (EE) of chitosan nanoparticles

Concentration (mg/ml)	Particle size (nm)	PDI	DL (%w/v)	EE (%)
0.5$	267.97 ± 5.3	0.46 ± 0.03	3.2 ± 0.4	28.9± 1.8
1	180.32 ± 4.2*	0.16 ± 0.01	10.1 ± 0.7	64.9 ± 1.5*

1.5	333.91 ± 4.9*	0.21 ± 0.03	9.2 ± 0.4	61.2± 1.0*
2	412.53 ± 7.9*	0.44 ± 0.07	8.7 ± 0.5	57.6 ± 1.2*
3	487.48 ± 10.4*	0.60 ± 0.05	7.0 ± 0.2	41.5 ± 3.5*

* p value< 0.05 when compared to control group $

Influence of chitosan to TPP ratio

Table 4 shows the effect of chitosan to sodium TPP ratio on particle size of nanoparticles formed. Particle size decreased significantly, when the ratio was varied from 2:1 to 4:1. On further increase in chitosan proportion, particle size also increased from 174.80 nm to 251.65 and 247.50 nm. Entrapment efficiency and drug loading of chitosan nanoparticles decreased linearly from 68.9% (with 2:1 chitosan to TPP ratio) to 44.31% (with 10:1 chitosan to TPP ratio) and 10.4±0.2 to 6.5±0.2 % respectively, although the change from 2:1 to 4:1 ratio was not found to be statistically significant. Similar type of trend was found in polyphenols encapsulation efficiency by varying chitosan-TPP mass ratio[11].

Table 4. Effect of chitosan to sodium TPP ratio on particle size, PDI, drug loading (DL) and entrapment efficiency (EE) of chitosan nanoparticles

Chitosan : TPP	Size (nm)	PDI	DL (%w/v)	EE (%)
2:1	505.27 ± 10.8*	0.42 ± 0.023	10.4 ± 0.2	68.90 ± 1.1
4:1$	174.80 ± 4.2	0.13 ± 0.01	10.3 ± 0.5	65.14 ± 2.1
8:1	251.65 ± 2.5*	0.19 ± 0.02	9.0 ± 0.4	53.73± 2.5*
10:1	247.50 ± 3.9*	0.12 ± 0.01	6.5 ± 0.2	44.31 ± 1.8*

* p value< 0.05 when compared to control group $

Influence of stirring speed

Table 5 shows the influence of stirring speed of magnetic stirrer on particle size and entrapment efficiency. Initially particle size decreased from 270.8 nm to 182.72 nm on increasing speed from 500 nm to 1000 nm, but on further increasing the speed, particle size increased linearly to 752.5 nm (at 2000 rpm). PDI also increased from 0.14 to 0.71. However in entrapment efficiency and drug loading, there was no statistically significant difference found on increasing the speed from 500 rpm to 2000 rpm. Polydispersity index of nanoparticles formed were low at 500 and 1000 rpm i.e. 0.13 and 0.14. On further increase in rpm polydispersity also increased. This is probably because adequate stirring can accelerate the dispersion of TPP in chitosan solution and increased shear force is helping to improve the monodispersity, while intense stirring at higher rpm may destroy the repulsive forces between nanoparticles and leads to aggregation of nanoparticles yielding increased particle size and PDI[174]. Therefore 1000 rpm was selected as the speed for further optimization.

Table 5. Effect of stirring speed on particle size, PDI, drug loading (DL) and entrapment efficiency (EE) of chitosan nanoparticles

Stirring speed	Particle size (nm)	PDI	DL (%w/v)	EE (%)
500	270.8± 5.5*	0.13 ± 0.02	10.9±0.4	65.3 ± 5.1
1000$	182.72± 6.2	0.14 ± 0.1	10.8±0.3	63.9± 3.7
1500	555.2 ±6.1*	0.62 ± 0.05	11.1±0.1	66.8± 4.5
2000	752.5±7.9*	0.71 ± 0.21	11.3±0.2	67.7 ± 3.8

* p value< 0.05 when compared to control group $

Influence of stirring time

At 1000 rpm, time of stirring was varied from 5 min to 30 min and its effect on nanoparticle size is presented in table 4.23. Both particle size and PDI did not vary significantly with stirring time. Also stirring time did not show significant effect on entrapment efficiency and drug loading of nanoparticles formed. Therefore at 1000 rpm stirring time of just 5 min was found to be sufficient and was selected for further optimization.

Table 6. Effect of stirring time on particle size, PDI, drug loading (DL) and entrapment efficiency (EE) of chitosan nanoparticles

Stirring Time	Particle size (nm)	PDI	DL (%w/v)	EE (%)
5$	179.15± 5.9	0.17 ± 0.015	10.9 ± 0.2	64.7 ± 2.5
10	177.43 ± 4.1	0.11 ± 0.012	10.4 ± 0.1	64.1 ± 3.2
10	177.43 ± 4.1	0.11 ± 0.012	10.4 ± 0.1	64.1 ± 3.2
30	170.25 ± 4.2	0.14 ± 0.013	11.1 ± 0.2	66.6 ± 3.5

* p value< 0.05 when compared to control group $

Therefore based on the optimization process chitosan and TPP concentration was finalized at 0.5 mg/ml, chitosan to TPP ratio 4:1, magnetic stirring at 1000 rpm just for five minutes was found to be sufficient.

Surface modification of chitosan nanoparticles

Alginate coating on chitosan nanoparticles

The chitosan nanoparticles so formed were further coated with alginate. Alginate being anionic polymer easily interacts with cationic chitosan molecules as well as its acid resistant properties make it suitable for controlled release of therapeutic molecules. Alginate coating of chitosan nanoparticles yielded nanoparticles of size 228.2 nm and 64.81% Rutaecarpine entrapment efficiency (Table 4.24). Successful coating of chitosan nanoparticles was confirmed by change in zeta potential and particle size of nanoparticles. FTIR of alginate sample and alginate coated chitosan nanoparticles also confirms the surface modification of chitosan nanoparticles. FTIR spectrum of alginate coated chitosan nanoparticles shows all the characteristic peaks of sodium alginate shown in Figure 4.10.

Table 7. Effect of alginate coating on particle size, PDI and zeta potential of chitosan nanoparticles

Formulation	Particle size (nm)	PDI	Zeta Potential (mV)
Uncoated chitosan NP	175.87±6.8	0.18 ± 0.02	+30.4
Alginate coated chitosan NP	228.22± 10.3	0.35 ± 0.05	-26.9

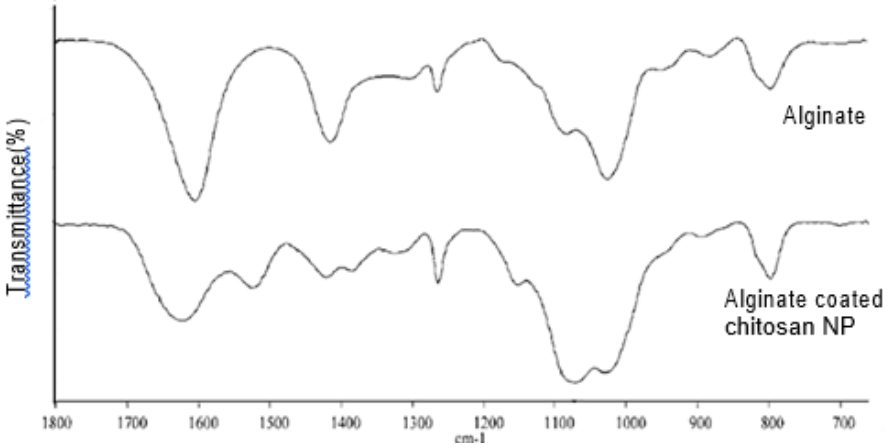

Figure 1. FTIR spectra of alginate and Rutaecarpine loaded alginate coated chitosan nanoparticles

Folic acid coating on chitosan nanoparticles

Chitosan nanoparticles were coated with folic acid for active targeting of nanoparticles. Folic acid is a low molecular weight vitamin whose receptors are frequently overexpressed in human cancer cells. As a targeting device to the tumor cells, folic acid presents a number of advantages. First, it is stable, inexpensive, nonimmunogenic compared to proteins such as monoclonal antibodies and compatible with organic solvents used during the preparation process. Secondly, folic acid binds to the folate receptors at cell surfaces with very high affinity and is internalized by receptor mediated endocytosis. Successful coating of chitosan nanoparticles was confirmed by change in zeta potential and particle size of nanoparticles (Table 8). FTIR spectrum of folic acid and folic acid coated chitosan nanoparticles also confirmed surface modification of chitosan nanoparticles. FTIR spectrum of folic acid coated chitosan nanoparticles showed all the characteristic peaks of folic acid as shown in Figure 4.11.

Table 8. Effect of folic acid coating on particle size, PDI and zeta potential of chitosan nanoparticles

Nanoparticles	Particle size (nm)	PDI	Zeta Potential (mV)
Uncoated Chitosan NP	175.87±6.8	0.18 ± 0.02	+30.4
Folic acid coated chitosan NP	198.51± 8.3	0.14 ± 0.01	+23.7

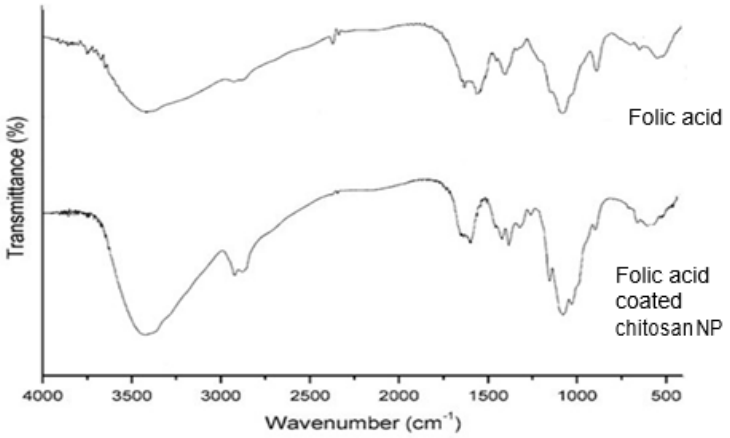

Figure 2. FTIR spectra of folic acid and folic acid coated Rutaecarpine loaded chitosan nanoparticles

SEM

Scanning electron microscopy has been widely used to provide surface and morphological information of the nanoparticles. The SEM images of both the coated formulations i.e. alginate coated chitosan nanoparticles and folic acid coated chitosan nanoparticles were obtained (Figure 4.12). Both types of coating provided spherical chitosan nanoparticles.

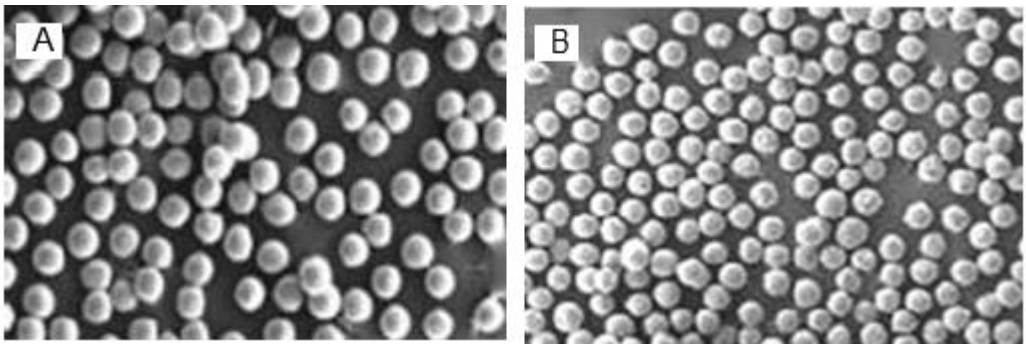

Figure 3. SEM images of alginate coated (A) and folic acid coated (B) chitosan nanoparticles.

Lyophilization of optimized formulation

Physical instability (aggregation/particle fusion) and/or chemical instability (hydrolysis of polymer materials forming the NP, drug leakage from nanoparticles and chemical reactivity of drug during the storage) contribute to the overall instability of the nanoparticulate uspension on long term storage. Hence, the improvement of NP stability represents an important issue in the development of these drug carriers. Freeze-drying appears as one of the most suitable methods to stabilize and facilitate the handling of colloidal systems, which otherwise stored as suspensions would suffer alteration in a brief period of time. Kreuter and Hartmann were among the first in reporting FD of polymeric nanoparticles, freeze drying of NP is a very elaborate and diligent process that requires a major investigation of the formulation and the process conditions. In the present study, FD studies were conducted using trehalose as lyoprotectant.

Table 9. Characterization of freeze dried cakes of coated optimized Rutaecarpine loaded chitosan nanoparticles

Formulation	**Cake texture**	**Moisture content(%w/w**	**Reconstitution**
Alginate coated chitosan NP	Intact and uniform cake	2.27± 0.23	Instantaneous
Folic acid coated chitosan NP	Intact and uniform cake	1.31± 0.17	Instantaneous

Table 10. Effect of lyophilization on particle size and PDI of of alginate coated and folic acid coated chitosan nanoparticles

Formulation	**Before Lyophilization**		**After Lyophilization**	
	Size(nm)	**PDI**	**size(nm)**	**PDI**
Alginate coated chitosan NP	230.14±11.2	0.37 ± 0.05	259.8 ± 12.9	0.42 ± 0.04
Folic acid coated chitosan NP	199.17± 9.7	0.14 ± 0.01	218.7 ± 10.2	0.20 ± 0.02

In vitro release profile

In vitro profiles of Rutaecarpine from uncoated chitosan nanoparticles, alginate coated chitosan nanoparticles and folic acid coated chitosan nanoparticles in phosphate buffer

(PBS, pH7.4) are shown in Figure 4.13. As depicted in Figure, the initial burst release (about 54%) of Rutaecarpine from uncoated chitosan nanoparticles was found in the first 24 h, followed by release of 95.5% in 7 days. The burst release might be attributed to the fact that Rutaecarpine molecules were loosely bound onto chitosan nanoparticles by ionic interaction which could be easily desorbed in ionic aqueous environment. Alginate coating onto chitosan nanoparticles decreased burst release of Rutaecarpine (21.55% release in 24h) but to a lesser extent than that by (10.55% release in 24h) folic acid coating. Overall rate of Rutaecarpine release was found to be higher from alginate coated chitosan NP than from folic acid coated chitosan NP, but the extent of Rutaecarpine released after 15 days was found to be the same (around 90%) from both the coated chitosan formulations.

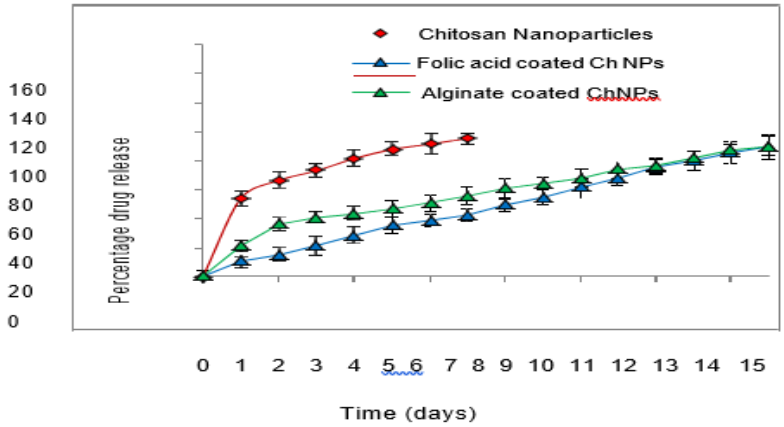

Figure 4. In vitro release of Rutaecarpine from chitosan nanoparticles and folic acid coated chitosan nanoparticles

Overall Rutaecarpine released from the coated chitosan nanoparticles was much less than that observed from uncoated chitosan nanoparticles. The longer release time and slower release rate of Rutaecarpine from coated chitosan nanoparticles might be explained by that there are strong interactions and additional coating layer could slow down the diffusion of Rutaecarpine from the system which also prolong the release time of Rutaecarpine from system. Due to both the degradation of coating and erosion of matrix, the Rutaecarpine might be released from the folic coated chitosan formulation in an extended release profile.

Storage stability

Evaluation of stability for long term storage conditions is deemed to be necessary. Here the changes in the physicochemical properties of Folic acid coated chitosan NPare

Physical appearance and reconstitution

It is important for lyophilized product that it should retain its all characteristics during storage and should perform like freshly prepared formulation at the time of its use. The optimized freeze dried product displayed no shrinkage at all the storage conditions over six months time period. Samples stored at 2-8°C were easily reconstituted in water even after of six months of storage but the samples stored at 40°C/75 % RH required manual shaking for reconstitution after 6 months of storage (Table 11).

i. Particle size and PDI

Samples stored at 2-8°C showed no significant change in particle size and PDI after six months of storage but the samples stored at 40°C/75 % RH showed significant increase in size from 217.2 nm to 627.6 nm and PDI from 0.106 to 0.819.

Table 11. Storage stability of Folic acid coated chitosan nanoparticles

Condition	Aspect	Reconstitution	Particle size (nm)	PDI	Drug loading (%w/v)
Fresh sample	Cake	Instantaneous	217.2 ± 9.7	0.106 ± 0.01	11.8 ± 0.2
After 1 month					
2-8°C	Cake	Instantaneous	216 ± 3.2	0.11 ± 0.02	11.5 ± 0.27
Ambient condition	Cake	Instantaneous	227 ± 10.2	0.11 ± 0.02	11.3 ± 0.23
40°C/75% RH	Cake	Instantaneous	269.3 ± 4.6	0.292 ± 0.07	9.4 ± 0.25
After 3 months					
2-8° C	Cake	Instantaneous	217.9 ± 2.1	0.118 ± 0.06	11.0 ± 0.25
Ambient condition	Cake	Instantaneous	222 ± 3.2	0.11 ± 0.02	10.5 ± 0.21
40° C/75% RH	Cake	Instantaneous	325.4 ± 1.4	0.479 ± 0.04	7.6 ± 0.27
After 6 months					
2-8° C	Cake	Instantaneous	219 ± 4.1	0.12 ± 0.07	10.8 ± 0.25
Ambient condition	Cake	Instantaneous	224.7 ± 3.2	0.14 ± 0.02	09.7 ± 0.22

40°C/75% RH	Cake	Manual shaking	627.6 ± 7.7	0.819 ± 0.04	05.42 ± 0.16

ii. Drug content

Rutaecarpine loading in folic acid coated chitosan NP did not change significantly at 2- 8°C and ambient conditions for six months of storage but at accelerated conditions(RH) Rutaecarpine loading decreased significantly after 1,3 and 6 months (Table 4.11).

pH stability Study

Table 12 shows the change in particle size and PDI of Rutaecarpine loaded folic acid coated chitosan NP after the incubation of nanoparticles for different time periods in different GIT fluids.

Table 12. Stability of Rutaecarpine loaded folic acid coated chitosan after exposure to simulated GIT media

Medium	Particle Size (mm)		PDI		Drug Loading(%w/v)	
	Initial	Final	Initial	Final	Initial	Final
pH 1.1		217.8 ± 10.2		0.106±0.02		11.7 ± 0.2
pH 3.5		216.5± 8.7		0.107±0.01		11.5 ± 0.2
pH 7.4	217.2 ± 9.7	218.1± 8.5	0.106 ± 0.01	0.109±0.02	11.8 ± 0.2	11.8 ± 0.2
SGF		219.7± 7.9		0.114±0.04		11.7 ± 0.2
SIF		220.9± 8.1		0.117±0.05		11.4 ± 0.2

The nanoparticlulate formulation was kept under acidic medium (pH 1.1, 3.5 and SGF) for 2h and in alkaline medium (pH 7.4 and SIF) for 6h. Particle size, PDI and drug loading did not differ significantly after incubating under stated conditions.

Hence, Folic acid coated chitosan nanoparticles were prepared using ionic gelation method which yielded nanoparticles of size around 217 nm, maximum Rutaecarpine entrapment efficiency around 65% and drug loading around 12%.So, this formulation was found to best among natural biodegradable polymers based nanoparticles and was selected for in vitro anticancer study.

CONCLUSION

Natural biodegradable polymer chitosan was used to formulate Rutaecarpine-loaded nanoparticles using ionic gelation method. Influence of different process variables (including chitosan concentration, sodium TPP concentration, chitosan to TPP ratio, stirring speed and time) on mean particle size, drug loading and entrapment efficiency of Rutaecarpine was determined and then the optimized chitosan nanoparticles were coated with alginate and folic acid. Optimized parameters were chitosan and TPP concentration 0.5 mg/ml, chitosan to TPP ratio 4:1, magnetic stirring at 1000 rpm just for five minutes was found to be sufficient. In vitro Rutaecarpine release profile from uncoated chitosan nanoparticles showed burst release (54% release) in initial 24 hours and complete release after about 7 days. Both alginate coating and folic acid coating on to chitosan nanoparticles decreased this initial burst release of Rutaecarpine from chitosan nanoparticles significantly, but folic acid coating decreased it to a much greater extent and it can be said that there was no burst release from folic acid coated formulation. Also both the coated chitosan formulations sustained the Rutaecarpine release profile from 7 days (of uncoated chitosan nanoparticles) to 15 days.. So, based on in vitro characterization and lyophilization of all the Rutaecarpine nanoparticulate formulations based on natural biodegradable polymers, folic acid coated chitosan nanoparticles were found to be the best for encapsulation of Rutaecarpine and was selected for in vitro anticancer study.

Funding - **Nil**

Conflicts of Interest - **The authors report no conflicts of interest in this work**

ACKNOWLEDGMENT

The authors thankfully acknowledge to the Department of Pharmaceutical Sciences, Vels Institute of Science, Technology and Advanced Studies (VISTAS), Pallavaram, Chennai-600117, Tamilnadu, India for providing facilities and continuous support throughout the study.

REFERENCES

i. Nagpal K, Singh SK, Mishra DN. Evaluation of safety and efficacy of brain targeted chitosan nanoparticles of minocycline. Int J Biol Macromol. 2013;59:20-8. doi: 10.1016/j.ijbiomac.2013.04.011, PMID 23587996.

ii. Wilson B, Samanta MK, Muthu MS, Vinothapooshan G. Design and evaluation of chitosan nanoparticles as novel drug carrier for the delivery of rivastigmine to treat Alzheimer's disease. Ther Deliv. 2011;2(5):599-609. doi: 10.4155/tde.11.21, PMID 22833977.

iii. Sarvaiya J, Agrawal YK. Chitosan as a suitable nanocarrier material for anti-Alzheimer drug delivery. Int J Biol Macromol. 2015;72:454-65. doi: 10.1016/j.ijbiomac.2014.08.052, PMID 25199867.

iv. Bowman K, Leong KW. Chitosan nanoparticles for oral drug and gene delivery. Int J Nanomedicine. 2006;1(2):117-28. doi: 10.2147/nano.2006.1.2.117, PMID 17722528.

v. Nikai T, Basbaum AI, Ahn AH. Profound reduction of somatic and visceral pain in mice by intrathecal administration of the anti-migraine drug, sumatriptan. Pain. 2008;139(3):533-40. doi: 10.1016/j.pain.2008.06.002, PMID 18723285.

vi. Bartsch T, Knight YE, Goadsby PJ. Activation of 5-HT (1B/1D) receptor in the periaqueductal gray

inhibits nociception. Ann Neurol. 2004;56(3):371-81. doi: 10.1002/ana.20193, PMID 15349864.

vii. Okamoto K, Thompson R, Tashiro A, Chang Z, Bereiter DA. Bright light produces Fos-positive neurons in caudal trigeminal brainstem. Neuroscience. 2009;160(4):858-64. doi: 10.1016/j.neuroscience.2009.03.003, PMID 19285114.

viii. Vijayan L, Bansal D, Ray SB. Nimodipine down-regulates CGRP expression in the rat trigeminal nucleus caudalis. Indian J Exp Biol. 2012;50(5):320-4. PMID 22803321.

ix. Landen JW, Hau V, Wang M, Davis T, Ciliax B, Wainer BH, Van Meir EG, Glass JD, Joshi HC, Archer DR. Rutaecarpine crosses the blood–brain barrier and inhibits glioblastoma growth. Clin Cancer Res. 2004;10(15):5187-201. doi: 10.1158/1078- 0432.CCR-04-0360, PMID 15297423.

x. Aneja R, Dhiman N, Idnani J, Awasthi A, Arora SK. Preclinical pharmacokinetics and bioavailability of Rutaecarpine, a tubulinbinding anticancer agent. Cancer Chemotherpharmacol. 2007;60:831-9.

xi. Gibaldi M, Weiner ND. Biphasic elimination of Rutaecarpine. J Pharm Sci. 1966;55(8):769-71. doi: 10.1002/jps.2600550804, PMID 5975287.

xii. Madan J, Dhiman N, Parmar VK, Sardana S, Bharatam PV, Aneja R, Chandra R, Katyal A. Inclusion complexes of Rutaecarpine in βcyclodextrin offer better solubility and improved pharmacokinetics. Cancer Chemother Pharmacol. 2010;65(3):537-48. doi: 10.1007/s00280-009-1060-3, PMID 19597818.